THE JOURNAL OF BIOLOGICAL CHEMISTRY VOL. 287, NO. 26, pp. 21615–21627, June 22, 2012

Functional Determinants of Human Enteric α-Defensin HD5

CRUCIAL ROLE FOR HYDROPHOBICITY AT DIMER INTERFACE[*S]

Received for publication, March 30, 2012, and in revised form, April 30, 2012 Published, JBC Papers in Press, May 9, 2012, DOI 10.1074/jbc.M112.367995

Mohsen Rajabi, Bryan Ericksen, Xueji Wu, Erik de Leeuw, Le Zhao[1], Marzena Pazgier[2], and Wuyuan Lu[3]

From the Institute of Human Virology and Department of Biochemistry and Molecular Biology, University of Maryland School of Medicine, Baltimore, Maryland 21201

Background: Human α-defensin HD5 is a multifunctional antimicrobial peptide whose functional determinants have yet to be elucidated.
Results: Alanine scanning mutagenesis aided by x-ray crystallography identified Leu[29] at the dimer interface as crucial; *N*-methylation of Glu[21] to debilitate HD5 dimerization also affected activity.
Conclusion: Dimerization and hydrophobicity are important for HD5 function.
Significance: The molecular basis of α-defensin function is better understood.

Human α-defensins are cationic peptides that self-associate into dimers and higher-order oligomers. They bind protein toxins, such as anthrax lethal factor (LF), and kill bacteria, including *Escherichia coli* and *Staphylococcus aureus*, among other functions. There are six members of the human α-defensin family: four human neutrophil peptides, including HNP1, and two enteric human defensins, including HD5. We subjected HD5 to comprehensive alanine scanning mutagenesis. We then assayed LF binding by surface plasmon resonance, LF activity by enzyme kinetic inhibition, and antibacterial activity by the virtual colony count assay. Most mutations could be tolerated, resulting in activity comparable with that of wild type HD5. However, the L29A mutation decimated LF binding and bactericidal activity against *Escherichia coli* and *Staphylococcus aureus*. A series of unnatural aliphatic and aromatic substitutions at position 29, including aminobutyric acid (Abu) and norleucine (Nle) correlated hydrophobicity with HD5 function. The crystal structure of L29Abu-HD5 depicted decreased hydrophobic contacts at the dimer interface, whereas the Nle-29-HD5 crystal structure depicted a novel mode of dimerization with parallel β strands. The effect of mutating Leu[29] is similar to that of a C-terminal hydrophobic residue of HNP1, Trp[26]. In addition, in order to further clarify the role of dimerization in HD5 function, an obligate monomer was generated by *N*-methylation of the Glu[21] residue, decreasing LF binding and antibacterial activity against *S. aureus*. These results further characterize the dimer interface of the α-defensins, revealing a crucial role of hydrophobicity-mediated dimerization.

Defensins are multifunctional peptides of innate immunity (1–5). These small, 2–5-kDa peptides are classified into α, β, and θ families based on sequence homology and the connectivity of disulfide bonds linking the six conserved cysteine residues (6, 7). Defensins bind carbohydrates (8, 9), lipids (10, 11), and DNA (12) and are active against a wide range of microorganisms, including bacteria (13, 14) and viruses (15–17). Defensins are also capable of interacting with an diverse array of cellular receptors and host proteins, playing important immunomodulatory functions (5, 18). In humans, six members of the α-defensin family have been described: human neutrophil peptides 1–4 (HNP1 to -4) present in the neutrophil granules (19–22) and human defensin 5 and 6 (HD5 and -6) secreted by the Paneth cells of the intestinal crypts (23, 24). Each of the six α-defensins is expressed with a pro-domain, which functions in sorting to the correct compartment, the inhibition of activity while the pro-peptide is still attached, and the facilitation of the correct folding of the mature defensin (25–31).

The exact mechanisms of defensin function are not fully understood. Human α-defensins kill Gram-positive bacteria preferentially to Gram-negative bacteria, suggesting a mode of action that depends upon bacterial physiology (14). The traditional view holds that electrostatic interactions and disruption of the bacterial membrane cause lethality, which appears to explain the sensitivity of the Gram-negative *Escherichia coli* (32). However, a recent study failed to find a correlation between α-defensin membrane activity and killing of the Gram-positive *Staphylococcus aureus*, instead attributing cell death to lipid II binding and sequestration (11), a mode of action reminiscent of the lantibiotic peptide nisin (33, 34) and other defensins (35–37). Defensins also neutralize secreted bacterial toxins and virulence factors (1, 38–42), including anthrax lethal toxin (43–45), which is a binary complex of two

* This work was supported, in whole or in part, by National Institutes of Health Grants AI072732 and AI061482 (to W. L.).
[S] This article contains supplemental Tables S1 and S2 and Fig. S1.
The atomic coordinates and structure factors (codes 4E86, 4E83, and 4E82) have been deposited in the Protein Data Bank, Research Collaboratory for Structural Bioinformatics, Rutgers University, New Brunswick, NJ (http://www.rcsb.org/).
[1] A Guanghua Scholar supported by Xi'an Jiaotong University School of Medicine.
[2] To whom correspondence may be addressed: Institute of Human Virology and Dept. of Biochemistry and Molecular Biology, University of Maryland School of Medicine, 725 W. Lombard St., Baltimore, MD 21201. E-mail: mpazgier@ihv.umaryland.edu.
[3] To whom correspondence may be addressed: Institute of Human Virology and Dept. of Biochemistry and Molecular Biology, University of Maryland School of Medicine, 725 W. Lombard St., Baltimore, MD 21201. E-mail: wlu@ihv.umaryland.edu.

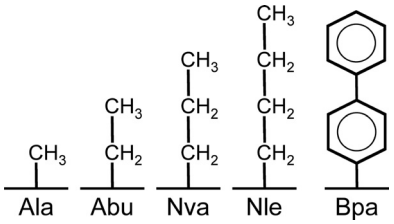

FIGURE 1. **Side chains of Ala and the non-coded amino acids Abu, Nva, Nle, and Bpa.**

proteins secreted by *B. anthracis*: lethal factor (LF)[4] and protective antigen (46). LF is a Zn^{2+}-dependent protease that induces cell death in macrophages through disruption of signaling pathways, and its inhibition has relevance for the development of therapies to treat anthrax exposure (47).

α-Defensins adopt a three-stranded β-sheet core structure stabilized by three intramolecular disulfides and associate into a dimer via their second β-strands (48, 49). The molecular basis of the myriad α-defensin functions is gradually being elucidated (1). Many of the prior studies have been focused on two model systems: HNP1 and α-defensins from mouse crypts, also known as cryptdins (50). Collectively, these studies have provided important insights into the structural and functional roles of disulfide bonding (51, 52), cationicity (53, 54), and conserved elements, such as the Arg-Glu salt bridge (55–58) and invariant Gly residue (59, 60) in the action of α-defensins. Recently, a comprehensive Ala scanning mutagenesis of HNP1 has discovered that a hydrophobic residue near the C terminus, Trp^{26}, governs the ability of this α-defensin to kill *Staphylococcus aureus*, inhibit anthrax lethal factor, and bind HIV-1 envelope glycoprotein gp120 (61); methylation of a peptide bond at the putative dimer interface of HNP1 debilitates its dimerization and is functionally detrimental (62). Despite structural conservation, mammalian α-defensins share rather limited sequence identity. Whether or not these findings seen with HNP1 can be generalized to other members of the α-defensin family remains to be tested.

The two enteric human α-defensins HD5 and HD6 play important roles in intestinal host defense and homeostasis (63). Although several structure-function relationship studies have been reported on HD5, focusing on disulfide bonding, the conserved salt bridge, and selective cationic and hydrophobic residues (8, 52, 56, 64–71), the molecular determinants of HD5 function remain largely unexplored. In the present study, an Ala scanning approach, aided by x-ray crystallography, enabled the thorough examination of the bactericidal properties and anthrax lethal factor inhibition of HD5 as a function of its sequence. Somewhat analogous to HNP1 Trp^{26}, HD5 Leu^{29} at the C terminus was identified as the most important residue. For functional interrogation, a series of hydrophobic amino acid substitutions were synthesized at position 29 using side chains of increasing aliphatic or aromatic chain length, including aminobutyric acid (Abu), norvaline (Nva), norleucine (Nle), Phe, and biphenylalanine (Bpa) (Fig. 1). To further study the effect of dimerization on HD5, Glu^{21} at the dimer interface was *N*-methylated to produce an obligate HD5 monomer. Together, these mutant forms of HD5 portrayed the influence of Leu^{29} and dimerization in the context of a richer understanding of the significance of hydrophobicity in the C-terminal region of the human α-defensins.

MATERIALS AND METHODS

Synthesis of HD5 and Mutant Analogues—The amino acid sequence of HD5 is as follows: ATCYCRTGRC^{10}ATRESLSGVC^{20}EISGRLYRLC^{30}CR^{32}. HD5 was synthesized as described previously (72). The same procedure was used to synthesize a set of HD5 molecules with a single alanine substitution at one of the positions in the sequence: T2A, Y4A, T7A, G8A, R9A, T12A, R13A, S15A, L16A, S17A, V19A, E21A, I22A, S23A, G24A, R25A, L26A, Y27A, R28A, and R32A. E21I-HD5 was also synthesized by this procedure. All of the cysteine residues (Cys^3, Cys^5, Cys^{10}, Cys^{20}, Cys^{30}, and Cys^{31}), an invariant glycine Gly^{18} (59, 60), two residues that form a structurally essential salt bridge (Arg^6 and Glu^{14}) (56), and the two native alanines (Ala^1 and Ala^{11}) were excluded from the mutagenesis. L29A-HD5 was synthesized as a pro-peptide following native chemical ligation with the HD5 pro-domain as described (56). The other L29*X*-HD5 mutants, L29Abu-HD5 (aminobutyric acid), L29Nva-HD5 (norvaline), L29Nle-HD5 (norleucine), L29F-HD5, and L29Bpa-HD5 (biphenylalanine) did not require ligation to the pro-peptide, and all were synthesized using the same procedure as HD5 (72). *N*-Methylated HD5, $MeGlu^{21}$-HD5, was prepared by replacing Glu^{21} with *N*-methyl-Glu in the HD5 synthesis procedure. All peptides were purified to homogeneity by C18 reversed-phase HPLC, and their molecular masses were verified by electrospray ionization MS. The quantification of defensins was done by UV measurements at 280 nm using molar extinction coefficients calculated from a published algorithm (73). Recombinant anthrax lethal factor was purchased from List Biological Laboratories, Inc. A sequence-optimized chromogenic substrate of lethal factor, Ac-NleKKKKVLP-*p*-nitroaniline, was synthesized as described (52).

Surface Plasmon Resonance (SPR)-based LF Binding—SPR experiments were performed on a BIAcore T100 system (BIAcore, Inc., Piscataway, NJ), unless stated otherwise, at 25 °C in 10 mM HEPES, 150 mM NaCl, 0.05% surfactant P20, pH 7.4 (with or without 3 mM EDTA). LF was immobilized on a CM5 sensor chip at a level of 2500 response units by the amine coupling protocol. Analytes were introduced into the flow cells at 30 μl/min in the running buffer. Association and dissociation were assessed for 5 and 10 min, respectively. Resonance signals were corrected for nonspecific binding by subtracting the background of the control flow cell. After each analysis, the sensor chip surfaces were regenerated with 10 mM glycine solution (pH 2.0) and 50 mM NaOH and equilibrated with the buffer before the next injection. Binding isotherms were analyzed with BIAevaluation software and/or GraphPad Prism.

LF Inhibition Kinetics—The inhibition of LF by various defensins was quantified using an enzymatic kinetic assay (52). Briefly, freshly prepared LF at a final concentration of 1 μg/ml (10 nM) was incubated at 37 °C for 30 min with a 2-fold dilution series of defensin in 20 mm HEPES buffer containing 1 mM

[4] The abbreviations used are: LF, lethal factor; SPR, surface plasmon resonance; Abu, aminobutyric acid; Nle, norleucine; Bpa, biphenylalanine; Nva, norvaline; H-bond, hydrogen bond; vLD, virtual lethal dose.

$CaCl_2$ and 0.5% Nonidet P-40, pH 7.2. 20 μl of LF substrate (1 mM) was added to each well to a final concentration of 100 μM in a total volume of 200 μl. The enzyme activity, characterized as a time-dependent absorbance increase at 405 nm due to the release of *p*-nitroaniline, was monitored at 37 °C over a period of 5 min on a 96-well V_{max} microplate reader (Molecular Dynamics, Inc.). Data are presented in a plot showing percentage inhibition *versus* defensin concentration, from which IC_{50} values (the concentration of defensin that reduced the enzymatic activity of LF by 50%) were derived by a non-linear regression analysis.

Virtual Colony Count—Antimicrobial assays against *E. coli* ATCC 25922 and *S. aureus* ATCC 29213 were conducted using a previously detailed 96-well turbidimetric method called "virtual colony count" (14). A 2-fold dilution series of defensin, ranging from 0.195 to 50 μM in 10 mM sodium phosphate, pH 7.4, plus 1% tryptic soy broth, was incubated at 37 °C for 2 h with *E. coli* or *S. aureus* (1×10^6 cfu/ml), followed by the addition of twice concentrated Mueller-Hinton broth. Kinetic measurements of bacterial growth at 650 nm over 12 h were taken using a V_{max} plate reader kept in a 37 °C room. Data analysis utilized a Visual Basic script to calculate the time necessary for each growth curve to reach a threshold change in optical density at 650 nm of 0.02. To increase the sensitivity of bacterial killing, the phosphate buffer used in the 2-h incubation period contained 1% tryptic soy broth, as was used previously for defensins (30, 52).

Crystallization, Data Collection, and Structure Determination—Crystallization screenings were conducted at room temperature using the hanging drop, vapor diffusion method and the commercially available crystallization Sparse Matrix Screens (Hampton Research). The drops were generated by mixing 0.5 μl of defensin solution (prepared at 20 mg/ml in water) with 0.5 μl of reservoir solution and placed over 0.8 ml of reservoir solution. The final compositions of the reservoir and cryosolutions are listed in supplemental Table S1. In all cases, the crystals appeared after 1 day and grew to their final sizes within a week. X-ray diffraction data were collected from flash-frozen crystals mounted on a rotating anode x-ray generator Rigaku-MSC Micromax 7 equipped with a Raxis-4++ image plate detector (at the X-ray Crystallography Core Facility, University of Maryland, Baltimore, MD) and at the Stanford Synchrotron Radiation Lightsource BL7–1 beamline on an ADSC QUANTUM 315 area detector. Crystal diffraction images were indexed, integrated, scaled, and merged using the HKL2000 package (74). The data collection statistics are shown in supplemental Table S2.

The structures of L29Abu-HD5, L29Nle-HD5, and $MeGlu^{21}$-HD5 were solved by molecular replacement using the program Phaser from the CCP4 suite (75) with the HD5 monomer as a search model (Protein Data Bank entry 1ZMP (48)). The structures were refined with the program Refmac (76), and the models were corrected by manually refitting into the electron density and rebuilt using the program COOT (77). The refinement results are summarized in supplemental Table S2. The coordinates and structure factors have been deposited in the Protein Data Bank with accession codes of 4E86, 4E83, and 4E82 for L29Abu-HD5, L29Nle-HD5, and $MeGlu^{21}$-HD5, respectively. Molecular graphics were generated using PyMOL (Schrodinger LLC, New York).

RESULTS

All Mutants Could Be Folded without Pro-domain Except for L29A-HD5—For this study, we synthesized and folded wild type HD5 and its 28 analogs, including 21 alanine scanning mutants, five L29*X*-HD5 mutants, one *N*-methylated peptide, $MeGlu^{21}$-HD5, and E21I-HD5. We excluded mutations of the six conserved cysteine residues and the invariant Gly^{18} as well as the salt bridge-forming residues Arg^6 and Glu^{14} because these residues ensure the structural integrity of HD5 and other α-defensins. We have previously established robust, facile synthesis and folding protocols for human α-defensins, which we employed to synthesize HD5 and all of its mutants except L29A. L29A could not be productively folded alone using the standard procedure, resulting in precipitation and a highly heterogeneous HPLC trace. However, α-defensin pro-domains have a chaperone-like effect on the oxidative folding of the mature defensin (30). Native chemical ligation (78, 79) between the defensin and its pro-domain followed by oxidation resulted in the correctly folded full-length pro-defensin (56). The pro-domain was subsequently removed via cyanogen bromide cleavage, leaving the folded defensin intact. All peptides were purified to homogeneity by preparatory HPLC, and their experimentally determined molecular masses were in agreement with the calculated values based on their average isotopic compositions (data not shown).

Alanine Scanning Mutations Point to Leu^{29} as Most Crucial Residue—We utilized SPR to assay the binding of the analogues to anthrax lethal factor. As shown in Fig. 2, wild type HD5 bound to LF with high affinity, as observed previously (52). Of all of the alanine scanning HD5 analogues tested, only S15A-HD5 bound to LF more efficiently. Interestingly, mutations of predominantly hydrophobic residues in the C-terminal region of the peptide, such as L26A, Y27A, and especially L29A, showed the weakest binding to LF of the panel of peptides. Also, mutations that reduced the net positive charge of the molecule (Arg-to-Ala substitutions) showed weaker binding compared with the wild type peptide only when residues were located toward the C terminus. For example, the R28A and R25A analogues showed weaker binding than R9A or R13A, with the final C-terminal R32A analog being the exception. Notably, the increase of cationicity due to the replacement of the single anionic residue in the sequence (E21A) also significantly reduced binding affinity for LF.

We have shown previously that wild type HD5 binds to and neutralizes the enzymatic activity of anthrax lethal factor or LF, a major virulence factor from *Bacillus anthracis* (52). We determined the effects of alanine mutations on the ability of HD5 to inhibit the enzymatic activity of LF. Fig. 2 shows the percentage residual LF activity as a function of the defensin concentration. Non-linear regression analysis was used to calculate the IC_{50} values, listed in Table 1. Wild type HD5 showed a higher IC_{50} value than the one reported previously (332 *versus* 192 nM) (52). As was the case for LF binding described above, most alanine scanning analogues inhibited LF activity comparably to the wild type peptide, as illustrated by only marginal differences in IC_{50}

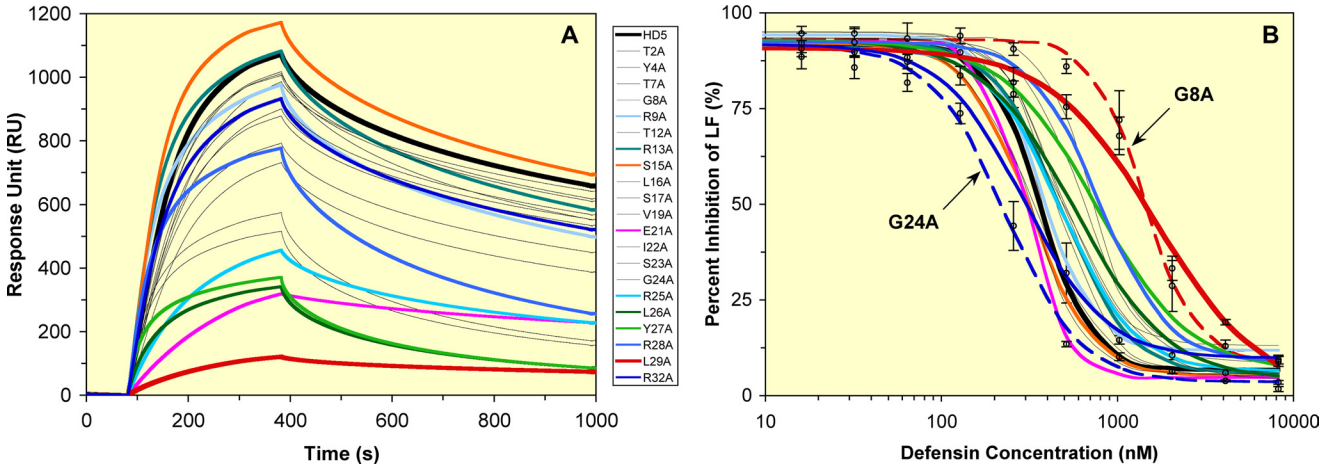

FIGURE 2. **LF binding and inhibition by HD5 and alanine scanning mutants.** *A*, representative binding kinetics of defensins, each at 200 nM, on immobilized LF (2500 response units) as determined by SPR. Wild type HD5 is highlighted with a *thick black line*, and the 10 *color-coded* HD5 analogs are R9A, R13A, S15A, E21A, R25A, L26A, Y27A, R28A, L29A (*red*), and R32A. *B*, inhibition of LF activity by different concentrations of defensin. The data are averages of three independent enzyme kinetic measurements. For clarity, only the inhibition curves of HD5 (*black*), G24A (*dotted blue line*), L29A (*red*), and G8A (*dotted red line*) are *highlighted* with *error bars*.

TABLE 1

IC_{50} values of LF inhibition by HD5, alanine scanning mutants, L29X mutants, and MeGlu[21]-HD5

HD5 variant	IC_{50}
	nM
Wild type HD5	332 ± 47
T2A	481 ± 78
Y4A	696 ± 82
T7A	370 ± 45
G8A	1418 ± 183
R9A	372 ± 45
T12A	453 ± 44
R13A	293 ± 39
S15A	316 ± 68
L16A	627 ± 58
S17A	318 ± 42
V19A	475 ± 32
E21A	301 ± 36
I22A	519 ± 130
S23A	338 ± 58
G24A	232 ± 46
R25A	477 ± 105
L26A	573 ± 148
Y27A	759 ± 190
R28A	790 ± 158
L29A	1672 ± 500
R32A	295 ± 64
L29Abu	501 ± 75
L29Nva	469 ± 90
L29Nle	477 ± 75
L29F	324 ± 47
L29Bpa	1027 ± 112
MeGlu[21]	750 ± 150

values. Also consistent with the binding results, LF activity inhibition was weakest for analogues mutated in the C-terminal region. Notably, of all peptides tested, the L29A analog showed the weakest ability to inhibit LF activity (IC_{50} = 1672 ± 500 nM). Unexpectedly, the G8A analog showed the second weakest LF inhibition (IC_{50} = 1418 ± 183 nM), suggesting that this glycine may be structurally significant. Previous studies highlighted the importance of a glycine corresponding to Gly[18] that is conserved in all of the human α-defensins (59, 60). With the exception of G8, these results suggest that the single alanine mutations that most severely affect LF interactions are near the C terminus. Furthermore, they suggest that a decrease in hydrophobicity is functionally deleterious for LF binding and inhibition of LF activity, more so than a decrease in cationicity.

We tested the bactericidal capacity of selected alanine scanning HD5 mutants, R9A, S17A, E21A, I22A, Y27A, and L29A, and also the E21I mutant, in which the negatively charged HD5 residue was replaced with the corresponding hydrophobic residue from the HNP1 sequence. Fig. 3 shows the survival of *E. coli* or *S. aureus* against HD5 and analogues ranging in concentration from 0.195 to 50 μM. Virtual lethal dose values are given in Table 2. As observed previously, *S. aureus* was more susceptible to HD5 than *E. coli* (14, 65). Strikingly, L29A-HD5 showed essentially no bactericidal activity against *S. aureus*, even at the highest concentration tested (50 μM), and showed reduced killing of *E. coli*. The decrease in the positive charge of R9A-HD5 attenuated killing against both strains, whereas the increase in cationicity of E21A-HD5 and E21I-HD5 enhanced killing. Y27A-HD5 had strongly reduced killing of *S. aureus* but not *E. coli*.

HD5 L29X Mutations Alter Mode of Dimerization and Emphasize Role of Hydrophobicity—The results of bacterial killing and the LF binding and inhibition experiments showed the importance of Leu[29] for HD5 function. To further examine the nature of side chain hydrophobicity for the functional activity of HD5 at this position, we introduced the unnatural amino acids α-aminobutyric acid (L29Abu-HD5), norvaline (L29Nva-HD5), and norleucine (L29Nle-HD5). Hydrophobicity of these analogues is progressively restored compared with the alanine substitution by increasing the length of the aliphatic side chain. Two additional analogues were prepared, L29F-HD5 and L29-Bpa-HD5 (biphenylalanine), to determine the effects of aromatic hydrophobicity. Interestingly, although it was necessary to synthesize the L29A analog as a pro-peptide, the other Leu[29] analogues, L29F, L29Bpa, L29Abu, L29Nva, and L29Nle, folded correctly without the need for ligation to the pro-peptide. All peptides were purified to homogeneity, and their respective molecular masses were verified by mass spectrometry.

In addition, to validate the structural changes introduced by Abu and Nle substitutions, we solved the x-ray structures of L29Abu-HD5 and L29Nle-HD5 by a molecular replacement approach at resolution 2.75 and 1.9 Å, respectively

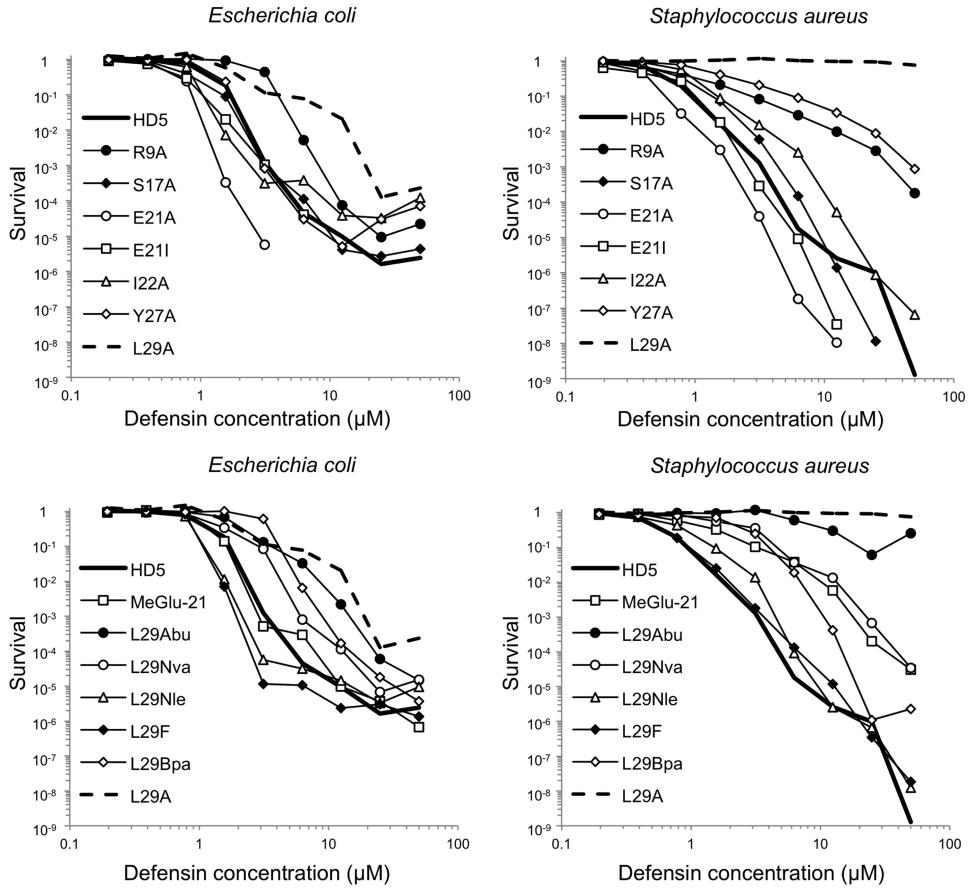

FIGURE 3. **Bactericidal activity of HD5 and analogues against *E. coli* and *S. aureus*.** Bacteria were treated with a 2-fold dilution series of each peptide from 0.195 to 50 μM. Each *curve* is the mean of triplicate ($n = 3$) experiments except HD5 *versus E. coli* ($n = 12$), HD5 *versus S. aureus* ($n = 9$), L29A *versus S. aureus* ($n = 9$), and E21A *versus S. aureus* at 6.25 μM ($n = 2$; an anomalous measurement was discarded). Zero survival cannot be plotted on a logarithmic scale. E21A-HD5 killed *E. coli* completely above 3.1 μM and *S. aureus* completely above 12.5 μM. E21I-HD5 killed *E. coli* completely above 6.3 μM and *S. aureus* completely above 12.5 μM. S17A-HD5 killed *S. aureus* completely at 50 μM.

TABLE 2

Antimicrobial virtual lethal doses (μM) that kill 50, 90, 99, and 99.9% of *E. coli* and *S. aureus*, as inferred using the virtual colony counting assay (7)

Defensin	*E. coli* ATCC 25922				*S. aureus* ATCC 29213			
	vLD_{50}	vLD_{90}	vLD_{99}	$vLD_{99.9}$	vLD_{50}	vLD_{90}	vLD_{99}	$vLD_{99.9}$
HD5[a]	1.2 ± 0.2	1.8 ± 0.2	2.1 ± 0.2	3.2 ± 0.5	0.53 ± 0.02	1.1 ± 0.07	2.0 ± 0.1	3.6 ± 0.3
R9A-HD5	3.0 ± 0.3	5.2 ± 0.2	6.4 ± 0.3	9.4 ± 1.7	0.74 ± 0.2	2.7 ± 0.8	9.2 ± 0.6	37 ± 6.9
S17A-HD5	0.78 ± 0.2	1.5 ± 0.5	2.0 ± 0.5	2.7 ± 1.2	0.67 ± 0.2	1.4 ± 0.4	2.8 ± 0.8	4.0 ± 1.0
E21A-HD5	0.62 ± 0.1	1.0 ± 0.2	1.5 ± 0.03	1.6 ± 0.002	0.41 ± 0.1	0.72 ± 0.02	1.0 ± 0.2	1.9 ± 0.5
E21I-HD5	0.66 ± 0.2	0.98 ± 0.3	1.7 ± 0.6	2.5 ± 1.0	0.48 ± 0.09	1.1 ± 0.3	1.7 ± 0.6	2.2 ± 0.7
MeGlu-21-HD5	1.2 ± 0.03	1.9 ± 0.2	2.9 ± 0.1	3.1 ± 0.01	1.2 ± 0.5	3.3 ± 1.2	10 ± 2.7	20 ± 3.4
I22A-HD5	0.88 ± 0.07	1.4 ± 0.03	1.8 ± 0.2	2.4 ± 0.4	0.85 ± 0.04	1.5 ± 0.02	4.1 ± 0.4	9.1 ± 1.0
Y27A-HD5	1.3 ± 0.1	2.2 ± 0.3	3.0 ± 0.1	3.6 ± 0.5	1.4 ± 0.3	6.0 ± 1.6	25 ± 5.9	41 ± 6.0
L29A-HD5[b]	1.8 ± 0.1	5.3 ± 1.4	11 ± 0.6	12 ± 0.07	>50	>50	>50	>50
L29Abu-HD5	2.0 ± 0.4	3.7 ± 0.9	9.7 ± 1.3	16 ± 3.4	12 ± 3.6	>50	>50	>50
L29Nva-HD5	1.5 ± 0.5	2.6 ± 1.1	3.5 ± 1.3	5.4 ± 1.7	2.5 ± 0.7	4.7 ± 1.1	12.7 ± 4.4	23 ± 7.2
L29Nle-HD5	0.96 ± 0.04	1.4 ± 0.02	1.8 ± 0.2	2.5 ± 0.5	0.75 ± 0.2	1.5 ± 0.4	3.5 ± 0.9	5.0 ± 1.0
L29F-HD5	1.0 ± 0.03	1.4 ± 0.01	1.7 ± 0.2	2.4 ± 0.3	0.53 ± 0.02	1.1 ± 0.06	2.4 ± 0.1	4.1 ± 0.6
L29Bpa-HD5	3.6 ± 0.7	4.9 ± 0.9	6.3 ± 0.5	9.9 ± 1.8	2.2 ± 0.05	4.9 ± 0.08	8.1 ± 1.1	12 ± 0.2

[a] 12 observations for *E. coli* and nine observations for *S. aureus*.
[b] Three observations for *E. coli* and nine observations for *S. aureus*.

(supplemental Table S2). L29A-HD5 also crystallized but diffracted poorly, and we were unable to solve the structure by molecular replacement. In all cases, a continuous and well defined electron density clearly confirmed the identity of each mutation as well as the connectivity of three disulfide bonds, which are identical with the wild type protein (Cys^3–Cys^{31}, Cys^5–Cys^{20}, and Cys^{10}–Cys^{30}) (Fig. 4). The tertiary structure is very well preserved among all structurally independent monomers of HD5 analogs, which are essentially identical to each other and to the wild type HD5 (Fig. 5). The root mean square deviations between 32 equivalent Cα atoms within monomers of HD5 analogs and wild type HD5 are in the range of 0.36–1.1 Å.

Analysis of intermolecular contacts within L29Abu-HD5 and L29Nle-HD5 crystals indicate that these analogs form stable but distinct dimers in the crystals (Fig. 6). L29Abu-HD5 monomers associate into dimers that are very similar to the

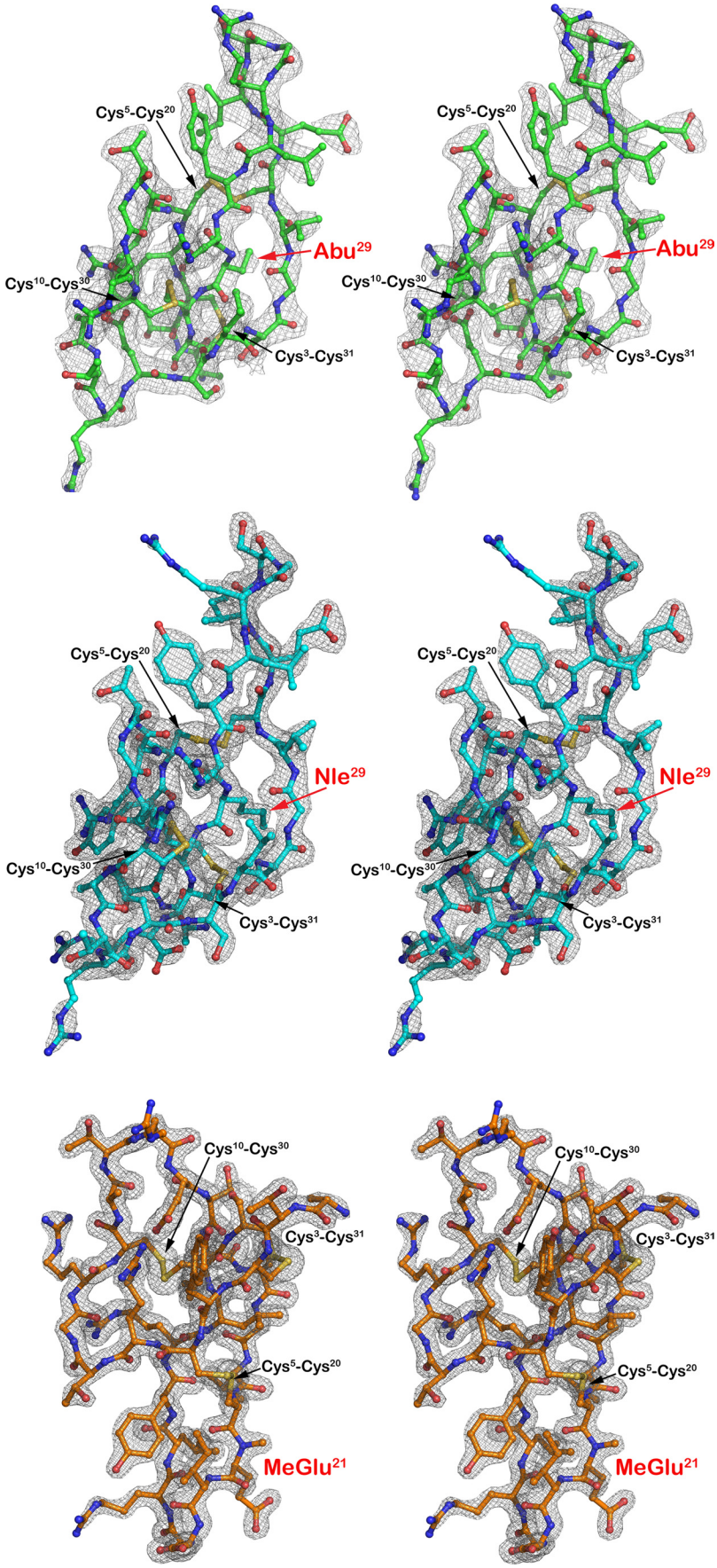
Cys5-Cys20
Abu29
Cys10-Cys30
Cys3-Cys31
Cys5-Cys20
Abu29
Cys10-Cys30
Cys3-Cys31
Cys5-Cys20
Nle29
Cys10-Cys30
Cys3-Cys31
Cys5-Cys20
Nle29
Cys10-Cys30
Cys3-Cys31
Cys10-Cys30
Cys3-Cys31
Cys5-Cys20
MeGlu21
Cys10-Cys30
Cys3-Cys31
Cys5-Cys20
MeGlu21

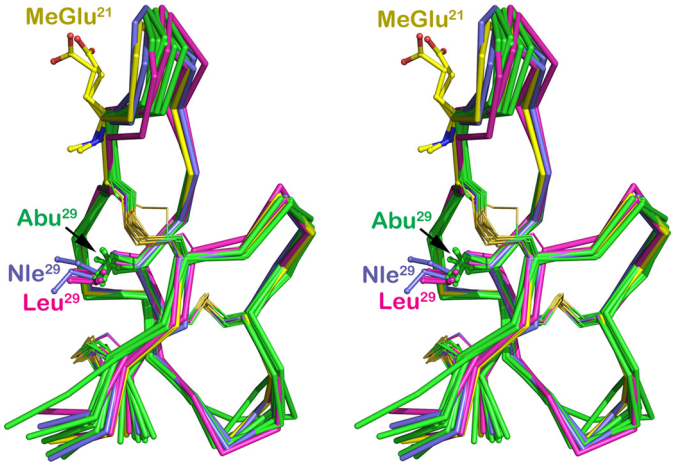

FIGURE 5. **Structural alignment of crystallographically independent monomers of HD5 analogs and wild type HD5.** Nine monomers present in the asymmetric unit of L29Abu-HD5 (*green*) crystal were aligned with two monomers of L29Nle-HD5 (*violet*), two monomers of MeGlu^{21}-HD5 (*yellow*), and four monomers of wild type HD5 (*magenta*) (Protein Data Bank entry 1ZMP (48)). Side chains of Leu^{29}, Abu^{29}, Nle^{29}, and MeGlu^{21} are shown in *ball-and-stick representations*, whereas backbone atoms are shown as *ribbons*. The superposition of monomers shows an extensive structural conservation of Cα atoms with minor fluctuations in the loop connecting the β1 and β2 strands and the β2-hairpin region.

canonical dimer of wild type HD5 (Fig. 6*A* and supplemental Fig. S1). The basket-shaped dimer is formed by the interaction of the long β2 strand of one monomer with the equivalent strand of the other monomer to form a four-stranded antiparallel β-sheet and the interaction of the short β1 strand of one monomer with the equivalent strand of the other monomer to form a two-stranded antiparallel β-sheet (Fig. 6*A*). The four-stranded sheet is stabilized by four backbone-backbone H-bonds donated reciprocally by Val^{19} nitrogen and Glu^{21} nitrogen of one monomer to Glu^{21} oxygen and Val^{19} oxygen of another, whereas the two-stranded sheet is maintained by two reciprocal backbone-backbone H-bonds formed by Cys^3 nitrogen and Cys^5 oxygen. The L29Abu-HD5 dimer is additionally stabilized through extensive hydrophobic interactions involving the side chain of Abu^{27} and the Cys^3–Cys^{31} disulfide of one monomer and the side chains of Ile^{22} and Tyr^{27} and the Cys^5–Cys^{20} disulfide of the opposite monomer (Fig. 6*A*, *middle*). Formation of this dimer results in the average burial of more than 431 Å^2 of molecular surface per monomer, which compares with an average of 399 Å^2 for the wild type HD5 dimer (Protein Data Bank entry 1ZMP (48)). The slight increase in the average value of the molecular surface buried within intermonomer interactions of L29Abu-HD5 as compared with the wild type dimer could be attributed to the presence of two, instead of one, N-terminal H-bonds formed between Cys^3 and Cys^5. Pairwise superposition of crystallographically independent dimers of L29Abu-HD5 and wild type HD5 indicates extensive structural conservation of all residues and results in an average distance between equivalent atoms in a range of 1.7–2.0 Å.

Two structurally independent monomers of the asymmetric unit of the L29Nle-HD5 crystal form a dimer that is topologically distinct from the "canonical" defensin dimer (Fig. 6*B*). L29Nle-HD5 monomers are arranged in a parallel fashion and form a four-stranded β-sheet by interaction of the β2 strand of one monomer with the β1 strand of another monomer. The dimerization is mediated through four hydrogen bonds formed between the backbone atoms of Val^{19} and Glu^{21} of the β2 strand and Ala^1 oxygen, Cys^3 nitrogen, Cys^3 oxygen, and Cys^5 nitrogen of the β1 strand (Fig. 6*B*, *left*) and hydrophobic contacts involving the side chains of Ile^{22}, Tyr^{27}, and Nle^{29} and Cys^{n1}–Cys^{n2} disulfides of each monomer (Fig. 6*B*, *middle* and *right*). The value of the molecular surface buried within intermonomer interactions was found to be 427 Å^2/monomer.

We examined the effects of the L29*X* substitutions in LF binding and inhibition using wild type HD5 and L29A as reference controls (Fig. 7 and Table 1). For LF binding, the relative binding affinities of the analogues ranked as follows, from lowest to highest: L29A-HD5 < L29Bpa-HD5 < L29Abu-HD5 < L29Nva-HD5 ~ L29Nle-HD5 ~ L29F-HD5 < HD5. Among the L29*X*-HD5 mutants, inhibition of LF activity was drastically altered only for the L29Bpa-HD5 peptide (IC_{50} = 1027 ± 112 *versus* 332 ± 47 nM for wild type).

We tested the bactericidal capacity of the L29Abu, L29Nva, L29Nle, L29F, and L29Bpa mutants (Fig. 3 and Table 2). L29F-HD5 was more active than HD5 against *E. coli* in the region of the virtual lethal doses and had activity against *S. aureus* similar to that of HD5. L29Bpa-HD5 was notably less active against both strains, with a $vLD_{99.9}$ of 9.9 μM *versus E. coli* and 12 μM *versus S. aureus* compared with HD5 with $vLD_{99.9}$ values of 3.2 and 3.6 μM, respectively. L29Abu-HD5 had little activity against *S. aureus* and less activity against *E. coli* than HD5. L27Nva-HD5 was less active against both strains. L29Nle-HD5 was more active against *E. coli* in the region of the virtual lethal dose values but less active against *S. aureus* in that region. In summary, aliphatic chain length is directly proportional to activity, and the single aromatic ring of phenylalanine gave better activity than the very bulky biphenylalanine side chain.

MeGlu^{21}-HD5 Crystallized as a Monomer and Had Decreased LF Binding Activity, LF Inhibition, and Activity against S. aureus but Not E. coli—MeGlu^{21}-HD5 was tested for its LF binding, LF-inhibiting, and antibacterial activity (Figs. 3 and 7 and Tables 1 and 2). MeGlu^{21}-HD5 was less effective at inhibiting LF compared with wild type, as evidenced by a more than 2-fold increase in LF inhibition assay IC_{50}, to 750 nM. LF binding was reduced 2.5-fold as measured by SPR. Against *E. coli*, MeGlu^{21}-HD5 activity was similar to HD5. However, against *S. aureus*, virtual lethal dose values differed by as much as 6-fold, with a $vLD_{99.9}$ of 20 μM for MeGlu^{21}-HD5 compared with 3.6 μM for HD5.

We determined the crystal structure of MeGlu^{21}-HD5 at 1.7 Å resolution and found the overall structure of the monomer not altered, presenting all of the previously identified secondary structure elements and resembling very closely the wild type HD5 (Fig. 5). Analysis of intermolecular contacts within the

FIGURE 4. **The final $2F_o - F_c$ electron density maps of HD5 analogs.** Maps are contoured at 1.5σ and are displayed around the entire molecule (monomer) of L29Abu-HD5 (*top*), L29Nle-HD5 (*middle*), and MeGlu^{21}-HD5 (*bottom*). Side chains of Abu^{29}, Nle^{29}, and MeGlu^{21} and disulfide bonds are *labeled*.

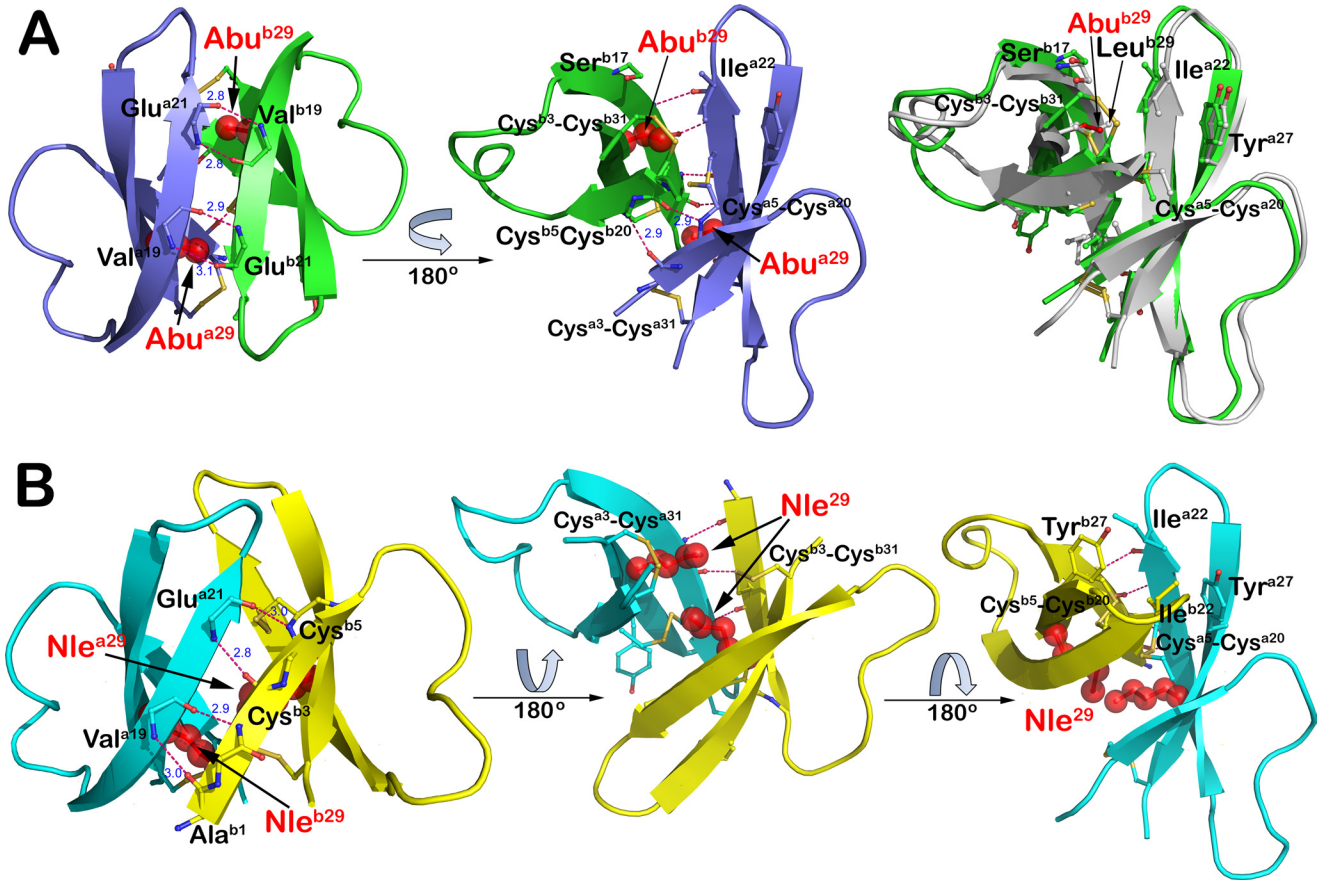

FIGURE 6. **Dimerization modes of HD5 analogs.** Dimeric assemblies of L29Abu-HD5 (*A*) and L29Nle-HD5 (*B*) are shown as observed in the crystal and structural alignment of L29Abu-HD5 and wild type HD5 dimers (*A*, *right*). Residues involved in dimer formation are shown in *ball-and-stick representations*. Main chain hydrogen bonds and their distances are *colored* in *magenta* and *blue*, respectively.

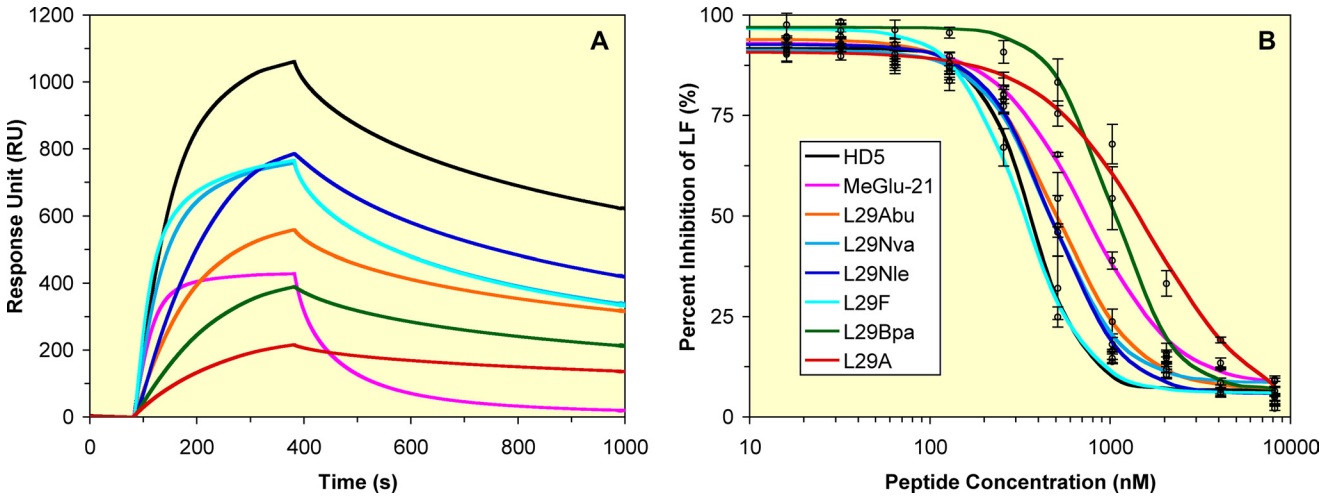

FIGURE 7. **LF binding and inhibition by HD5 and L29*X* mutants.** *A*, representative binding kinetics of defensins, each at 200 nM, on immobilized LF (2500 response units) as determined by SPR. *B*, inhibition of LF activity by different concentrations of defensin. The data are averages of three independent enzyme kinetic measurements, and the IC_{50} values are tabulated in Table 1.

MeGlu^{21}-HD5 crystal unambiguously rules out the formation of any quaternary structure. In this regard, monomers of MeGlu^{21}-HD5 closely resemble dimerization-impaired MeIle^{20}-HNP1 monomers (62). The MeGlu^{21}-HD5 crystal structure once again validates the utility of the employed *N*-methylation method of the defensins' design, forcing the defensins to be represented in the crystal as monomers.

DISCUSSION

There are at least two distinct roles of hydrophobicity in the mechanism of α-defensins. One is that an amphiphilic structure is induced upon membrane binding with hydrophobic surfaces exposed for membrane penetration. Another is that hydrophobicity maintains the dimeric inter-

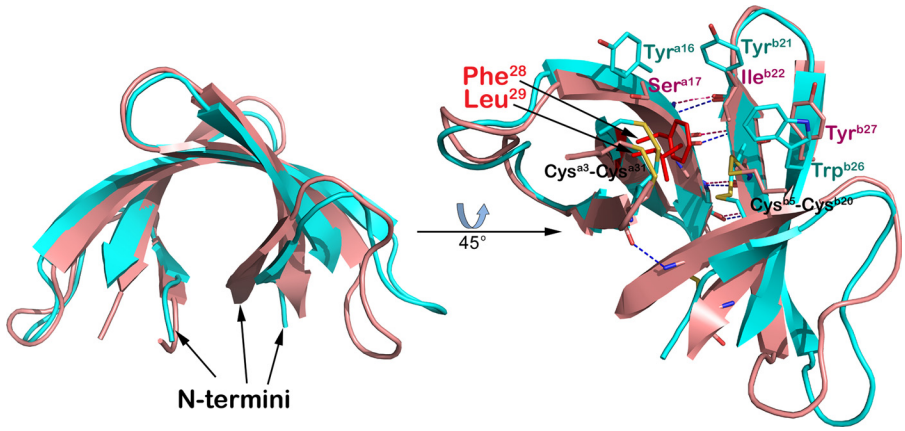

FIGURE 8. **Comparison of HD5 and HNP1 dimers.** Dimers were aligned based on monomer A and *colored pink* (HD5, Protein Data Bank entry 1ZMP (48)) and *cyan* (HNP1, Protein Data Bank 1GNY (52)). Backbone atoms are shown as *ribbons* (*left*) and rotated 45° to show details of the dimer interface (*right*). Side chains of residues involved in hydrophobic packing are shown as *sticks*. H-bonds stabilizing monomer-monomer associations are shown as *dashes* and *colored* in *blue* (HD5) and in *magenta* (HNP1). Note that canonical dimers of HD5 and HNP1 are symmetric and stabilized by two sets of hydrophobic interactions contributed by the equivalent residues of two monomers. Here only one set is shown for clarity.

face between defensin subunits. Our results emphasize the latter role.

Two biochemical underpinnings for defensin binding and activity are electrostatic attraction and the hydrophobic effect. The importance of positive charge in bacterial killing by defensins and their murine orthologues the cryptdins, viewed as essential for electrostatic interaction with the anionic bacterial membrane, is experimentally well supported (53, 54, 64). In further support, anionic residues in the pro-domain of cryptdins prevent their antibacterial activity (80–82), although more recent studies point to hydrophobicity of the pro-domain as the major factor governing the intramolecular functional inhibition of proHNPs (29). Although the interplay of cationicity and hydrophobicity clearly dictates defensin function, growing evidence suggests that the latter plays a dominant role in the action of human neutrophil α-defensins HNP1 to -3 (61), which are significantly less cationic than cryptdins or typical β-defensins. The work described in this report on HD5 lends additional support to the findings seen with human neutrophil peptides and underscores the importance of hydrophobicity for human α-defensin function.

We find that C-terminal hydrophobic residues of HD5, and in particular Leu^{29}, are important for its bactericidal activity. Substitution of Leu by Ala abolished *S. aureus* killing and severely decreased *E. coli* killing. The lost bactericidal activity of L29A-HD5 against both strains progressively improved as the hydrophobicity of residue 29 in L29*X*-HD5 (where *X* represents Abu, Nva, Nle, or Phe) increased, and both Nle and Phe were improvements over Leu against *E. coli*. Similarly, L29A was the most deleterious mutation for LF binding and inhibition by HD5, and the L29F mutation fully rescued the lost function of L29A-HD5 against LF. These results are in accordance with those previously reported for W26*X*-HNP1 analogs (61). Because both Trp^{26} (HNP1) and Leu^{29} (HD5) are bulky hydrophobic residues near the C termini of the respective defensins, they point to hydrophobicity, rather than cationicity, as the keystone of human α-defensin activity.

Members of the α-defensin family from several species (human, mouse, rhesus macaque, rabbit, guinea pig, and rat) commonly contain Leu or Phe at the position just before the fifth and sixth cysteines (55), which corresponds to Leu^{29} of HD5 or Phe^{28} of HNP1. Not surprisingly, in the previously published Ala scanning mutagenesis of HNP1 (61), the F28A mutation was the second most deleterious for bactericidal activity against *S. aureus*, next to W26A. However, because Tyr^{27} of HD5 corresponds to Trp^{26} of HNP1, the question remains; why is the Y27A mutation substantially less detrimental than the L29A mutation in HD5 and the W26A or F28A mutation in HNP1? The answer probably lies in differences in the mode of dimerization between the two α-defensins HNP1 and HD5 (Fig. 8) as well as different hydrophobicities of Leu, Phe, Tyr, and Trp residues.

Structural analysis of the HNP1 dimer indicates that Trp^{26} in each monomer stacks against Tyr^{21}, which, in turn, makes hydrophobic interactions with Phe^{28} of the opposing monomer, among others (62). The dimer is also stabilized by four reciprocal backbone H-bonds formed by Thr^{18} and Ile^{20}. According to the Wimley-White whole-residue hydrophobicity scale (water-octanol) (83, 84), Trp is more hydrophobic than Phe, with Tyr being the least hydrophobic among the three aromatic residues. Thus, Trp^{26} and, to a lesser extent, Phe^{28} prominently mediate HNP1 dimerization, which strongly correlates with defensin activity (61, 62). Compared with HNP1, however, the C terminus of HD5 is significantly more polar, and the only aromatic residue in the region, Tyr^{27} (corresponding to Trp^{26} in HNP1), does not directly participate in dimer formation as shown in the crystal structure of HD5 (48). In fact, the dimer interface of HD5 is formed mainly by Ser^{17}, Leu^{29}, and the Cys^{3}–Cys^{31} disulfide bond of one monomer, which pack against the Cys^{5}–Cys^{20} disulfide bond and Ile^{22} of the opposing monomer. On the Wimley-White whole-residue hydrophobicity scale, Leu is still more hydrophobic than Tyr, albeit less than Phe and Trp (83, 84). It is therefore not surprising that Leu^{29} was found to be more important than Tyr^{27} for HD5 function despite the fact that the latter and Trp^{26} of HNP1 occupy equivalent positions in the amino acid sequences. Of note, the difference in hydrophobicity between Leu and Trp may provide a ready explanation for the finding that W26A-HNP1 showed a

greater decrease in LF binding and inhibition than L29A-HD5 compared with the respective wild type peptides. W26A-HNP1 decreased the inhibition of LF enzymatic activity 19-fold compared with wild type HNP1, whereas L29A-HD5 decreased the inhibition of LF activity only 5-fold compared with HD5.

As is the case with Trp^{26} in HNP1, the functional importance of Leu^{29} probably stems from its prominent role in mediating HD5 dimerization, contributed additionally by four reciprocal intermolecular backbone-backbone H-bonds involving Val^{19} and Glu^{21}. This has been confirmed at both the structural and functional levels by methylation of the Cys^{20}–Glu^{21} peptide bond to debilitate HD5 dimerization. In fact, $MeGlu^{21}$-HD5 crystallized as an obligate monomer, and its bactericidal activity against *S. aureus* and inhibition of LF were attenuated in a similar way to the corresponding mutant of HNP1, $MeIle^{20}$-HNP1, as was recently reported (62). However, the deleterious effects of HD5 methylation at Glu^{21} are much smaller than those seen with $MeIle^{20}$-HNP1. The decrease in activity of $MeGlu^{21}$-HD5 compared with HD5 was 6-fold against *S. aureus*, as measured by $vLD_{99.9}$. By contrast, $MeIle^{20}$-HNP1 did not achieve 99 or 99.9% killing of *S. aureus*, resulting in vLD_{99} and $vLD_{99.9}$ values of >50 μM. Similarly, although $MeIle^{20}$-HNP1 had an 11-fold greater IC_{50} than HNP1 with respect to LF inhibition, $MeGlu^{21}$-HD5 had only a 2-fold increase in IC_{50} (750 nM) compared with HD5 (332 nM). Thus, dimerization appears to be functionally more important for HNP1 than HD5.

Compared with HNP1, the attenuated functional effects of the L29A mutation and Glu^{21} methylation in HD5 probably underscore differences in the mode of dimerization between HNP1 and HD5. In contrast to the HNP1 dimer, which is stabilized by only four reciprocal intermolecular backbone-backbone H-bonds, the HD5 dimer is stabilized additionally by one H-bond formed by the N-terminal backbone atoms of Cys^3. This additional H-bond contributes significantly to the solvation energy gain of the interface. These differences of dimerization features are well revealed by structural studies of L29Abu-HD5 and the previously published W26Abu-HNP1 (61). The W26Abu mutation caused little change to HNP1 tertiary and quaternary structures except for an increased local structural mobility of Tyr^{21} at the dimer interface (61). By contrast, the L29Abu mutation slightly increased the surface area buried at the dimer interface of HD5 due to enhanced intermolecular interactions of N termini accompanied by a conformational adjustment. This subtle but favorable structural change presumably offsets, at least partially, the deleterious mutational effects of L29Abu at the functional level. These structural findings also suggest that molecular defects at the dimer interface of HD5 may be functionally tolerable. Indeed, the L29Nle mutation caused a dramatic switch of the HD5 dimer from the (canonical) anti-parallel mode to a (non-canonical) parallel mode to avoid steric clashes at the dimer interface involving the elongated side chains of Nle-29. Despite this marked change in the mode of dimerization, L29Nle-HD5 had *S. aureus*-killing and LF-inhibiting/binding activities comparable with the wild type defensin HD5. Of note, in contrast to HNP1, structural plasticity seen in HD5 dimerization presumably makes it difficult to accurately predict its activity on the basis of its tendency to dimerize, oligomerize, or multimerize.

Leu-Leu interactions appear in protein motifs that stabilize dimeric structures, such as Leu-rich repeats (85) and Leu zippers (86), to achieve specific binding to ligands such as DNA. This general hydrophobic property of Leu is exploited in HD5 on a much smaller scale, where a pair of Leu^{29} side chains interact indirectly through the hydrophobic patch of the dimer interface. Changing Leu^{29} to Ala might have thermodynamic consequences similar to those of Leu-to-Ala substitutions that cause cavities within the hydrophobic core of T4 lysozyme (87, 88) or Leu zippers (89). The "cavities" in the case of L29A-HD5 would lie at the dimer interface, where the absence of the van der Waals contacts of the bulky Leu side chain might greatly decrease its hydrophobic surface area or eliminate dimerization altogether. Quite possibly, the Abu side chain might be the shortest permissible that provides sufficient hydrophobicity. Indeed, mutating Leu^{29} to the smaller and less hydrophobic Ala caused aggregation and misfolding, which was only alleviated through the chaperone-like pro-peptide. Replacing Leu^{29} with larger hydrophobic side chains, however, resulted in productively folded peptides. The series of L29*X* mutations of increasing hydrophobicity had self-association and activity proportional to side chain size with the exception of the extremely bulky Bpa. The results with Bpa indicate that there is a limit to the beneficial effect of hydrophobicity; a side chain much bulkier than that of Leu apparently cannot be accommodated by the defensin dimer without steric clashes.

Finally, unlike *S. aureus*, *E. coli* killing by HD5 or HNP1 was more sensitive to the change in cationicity than hydrophobicity. Moreover, $MeGlu^{21}$-HD5 activity was comparable with HD5 activity against *E. coli*, indicating that *E. coli* killing is independent of defensin dimerization. We and others have shown that a number of Gram-negative bacterial strains can be killed effectively independent of α-defensin structure and chirality (1). The present study further underscores the mechanistic difference in the bactericidal activity of α-defensins against these two bacterial strains, one mediated by achiral electrostatic attractions, such as to membrane phosphate groups, and the other mediated partially by hydrophobic interactions that result in specific binding to molecules, such as lipid II. Thus, strain selectivity could be explained by differences in defensin binding as it relates to the physiology of the bacterial cell wall and inner or outer membranes.

In summary, the results obtained from the comprehensive alanine scanning mutagenesis and the series of L29*X* mutations have identified hydrophobicity as the dominant functional trait, more important than cationicity (as shown by the selection of L29A over arginine mutations) and even more important than canonical dimerization (as shown by the relatively mild effects of monomerization in the $MeGlu^{21}$-HD5 mutant and the reorientation of the quite functional L29Nle-HD5 dimer). Disrupting dimerization appears to be less deleterious for HD5 than for HNP1, which also forms multimers that have been modeled to be governed by Ile^{20} and Leu^{25} (62). Despite the variation in the importance of quaternary structure among the human α-defensins, hydrophobicity-mediated α-defensin dimerization, oligomerization, and multimerization appear to

be an overriding molecular event that governs the great variety of biological activities of these multifunctional peptides.

Acknowledgments—We thank Drs. Changyou Zhan, Gang Wei, and Guozhang Zou and Weirong Yuan for technical assistance and useful discussions. We thank the X-ray Crystallography Core Facility of the University of Maryland at Baltimore for providing crystallographic equipment and resources. Portions of this research were carried out at the Stanford Synchrotron Radiation Lightsource, a Directorate of the SLAC National Accelerator Laboratory and an Office of Science User Facility operated for the United States. Department of Energy Office of Science by Stanford University. The Stanford Synchrotron Radiation Lightsource Structural Molecular Biology Program is supported by the Department of Energy Office of Biological and Environmental Research and by the National Institutes of Health, National Center for Research Resources, Biomedical Technology Program (Grant P41RR001209), and NIGMS, National Institutes of Health.

REFERENCES

1. Lehrer, R. I., and Lu, W. (2012) α-Defensins in human innate immunity. *Immunol. Rev.* **245,** 84–112
2. Ganz, T. (2003) Defensins. Antimicrobial peptides of innate immunity. *Nat. Rev. Immunol.* **3,** 710–720
3. Zasloff, M. (2002) Antimicrobial peptides of multicellular organisms. *Nature* **415,** 389–395
4. Selsted, M. E., and Ouellette, A. J. (2005) Mammalian defensins in the antimicrobial immune response. *Nat. Immunol.* **6,** 551–557
5. Yang, D., Biragyn, A., Hoover, D. M., Lubkowski, J., and Oppenheim, J. J. (2004) Multiple roles of antimicrobial defensins, cathelicidins, and eosinophil-derived neurotoxin in host defense. *Annu. Rev. Immunol.* **22,** 181–215
6. Hughes, A. L. (1999) Evolutionary diversification of the mammalian defensins. *Cell Mol. Life Sci.* **56,** 94–103
7. Pazgier, M., Hoover, D. M., Yang, D., Lu, W., and Lubkowski, J. (2006) Human β-defensins. *Cell Mol. Life Sci.* **63,** 1294–1313
8. Lehrer, R. I., Jung, G., Ruchala, P., Andre, S., Gabius, H. J., and Lu, W. (2009) Multivalent binding of carbohydrates by the human α-defensin, HD5. *J. Immunol.* **183,** 480–490
9. Wang, W., Cole, A. M., Hong, T., Waring, A. J., and Lehrer, R. I. (2003) Retrocyclin, an antiretroviral θ-defensin, is a lectin. *J. Immunol.* **170,** 4708–4716
10. Wimley, W. C., Selsted, M. E., and White, S. H. (1994) Interactions between human defensins and lipid bilayers. Evidence for formation of multimeric pores. *Protein Sci.* **3,** 1362–1373
11. de Leeuw, E., Li, C., Zeng, P., Li, C., Diepeveen-de Buin, M., Lu, W. Y., Breukink, E., and Lu, W. (2010) Functional interaction of human neutrophil peptide-1 with the cell wall precursor lipid II. *FEBS Lett.* **584,** 1543–1548
12. Hazrati, E., Galen, B., Lu, W., Wang, W., Ouyang, Y., Keller, M. J., Lehrer, R. I., and Herold, B. C. (2006) Human α- and β-defensins block multiple steps in herpes simplex virus infection. *J. Immunol.* **177,** 8658–8666
13. Lehrer, R. I., Lichtenstein, A. K., and Ganz, T. (1993) Defensins. Antimicrobial and cytotoxic peptides of mammalian cells. *Annu. Rev. Immunol.* **11,** 105–128
14. Ericksen, B., Wu, Z., Lu, W., and Lehrer, R. I. (2005) Antibacterial activity and specificity of the six human α-defensins. *Antimicrob. Agents Chemother.* **49,** 269–275
15. Klotman, M. E., and Chang, T. L. (2006) Defensins in innate antiviral immunity. *Nat. Rev. Immunol.* **6,** 447–456
16. Ding, J., Chou, Y. Y., and Chang, T. L. (2009) Defensins in viral infections. *J. Innate Immun.* **1,** 413–420
17. Penberthy, W. T., Chari, S., Cole, A. L., and Cole, A. M. (2011) Retrocyclins and their activity against HIV-1. *Cell Mol. Life Sci.* **68,** 2231–2242
18. Rehaume, L. M., and Hancock, R. E. (2008) Neutrophil-derived defensins as modulators of innate immune function. *Crit. Rev. Immunol.* **28,** 185–200
19. Gabay, J. E., Scott, R. W., Campanelli, D., Griffith, J., Wilde, C., Marra, M. N., Seeger, M., and Nathan, C. F. (1989) Antibiotic proteins of human polymorphonuclear leukocytes. *Proc. Natl. Acad. Sci. U.S.A.* **86,** 5610–5614
20. Wilde, C. G., Griffith, J. E., Marra, M. N., Snable, J. L., and Scott, R. W. (1989) Purification and characterization of human neutrophil peptide 4, a novel member of the defensin family. *J. Biol. Chem.* **264,** 11200–11203
21. Selsted, M. E., Harwig, S. S., Ganz, T., Schilling, J. W., and Lehrer, R. I. (1985) Primary structures of three human neutrophil defensins. *J. Clin. Invest.* **76,** 1436–1439
22. Ganz, T., Selsted, M. E., Szklarek, D., Harwig, S. S., Daher, K., Bainton, D. F., and Lehrer, R. I. (1985) Defensins. Natural peptide antibiotics of human neutrophils. *J. Clin. Invest.* **76,** 1427–1435
23. Jones, D. E., and Bevins, C. L. (1992) Paneth cells of the human small intestine express an antimicrobial peptide gene. *J. Biol. Chem.* **267,** 23216–23225
24. Jones, D. E., and Bevins, C. L. (1993) Defensin-6 mRNA in human Paneth cells. Implications for antimicrobial peptides in host defense of the human bowel. *FEBS Lett.* **315,** 187–192
25. Valore, E. V., Martin, E., Harwig, S. S., and Ganz, T. (1996) Intramolecular inhibition of human defensin HNP-1 by its propiece. *J. Clin. Invest.* **97,** 1624–1629
26. Ghosh, D., Porter, E., Shen, B., Lee, S. K., Wilk, D., Drazba, J., Yadav, S. P., Crabb, J. W., Ganz, T., and Bevins, C. L. (2002) Paneth cell trypsin is the processing enzyme for human defensin-5. *Nat. Immunol.* **3,** 583–590
27. Porter, E. M., Liu, L., Oren, A., Anton, P. A., and Ganz, T. (1997) Localization of human intestinal defensin 5 in Paneth cell granules. *Infect. Immun.* **65,** 2389–2395
28. Wu, Z., Prahl, A., Powell, R., Ericksen, B., Lubkowski, J., and Lu, W. (2003) From pro defensins to defensins. Synthesis and characterization of human neutrophil pro α-defensin-1 and its mature domain. *J. Pept. Res.* **62,** 53–62
29. Zou, G., de Leeuw, E., Lubkowski, J., and Lu, W. (2008) Molecular determinants for the interaction of human neutrophil alpha defensin 1 with its propeptide. *J. Mol. Biol.* **381,** 1281–1291
30. Wu, Z., Li, X., Ericksen, B., de Leeuw, E., Zou, G., Zeng, P., Xie, C., Li, C., Lubkowski, J., and Lu, W. (2007) Impact of pro segments on the folding and function of human neutrophil α-defensins. *J. Mol. Biol.* **368,** 537–549
31. Valore, E. V., and Ganz, T. (1992) Posttranslational processing of defensins in immature human myeloid cells. *Blood* **79,** 1538–1544
32. Lehrer, R. I., Barton, A., Daher, K. A., Harwig, S. S., Ganz, T., and Selsted, M. E. (1989) Interaction of human defensins with *Escherichia coli*. Mechanism of bactericidal activity. *J. Clin. Invest.* **84,** 553–561
33. Breukink, E., Wiedemann, I., van Kraaij, C., Kuipers, O. P., Sahl, H., and de Kruijff, B. (1999) Use of the cell wall precursor lipid II by a pore-forming peptide antibiotic. *Science* **286,** 2361–2364
34. Hasper, H. E., Kramer, N. E., Smith, J. L., Hillman, J. D., Zachariah, C., Kuipers, O. P., de Kruijff, B., and Breukink, E. (2006) An alternative bactericidal mechanism of action for lantibiotic peptides that target lipid II. *Science* **313,** 1636–1637
35. Schmitt, P., Wilmes, M., Pugnière, M., Aumelas, A., Bachère, E., Sahl, H. G., Schneider, T., and Destoumieux-Garzón, D. (2010) Insight into invertebrate defensin mechanism of action. Oyster defensins inhibit peptidoglycan biosynthesis by binding to lipid II. *J. Biol. Chem.* **285,** 29208–29216
36. Schneider, T., Kruse, T., Wimmer, R., Wiedemann, I., Sass, V., Pag, U., Jansen, A., Nielsen, A. K., Mygind, P. H., Raventós, D. S., Neve, S., Ravn, B., Bonvin, A. M., De Maria, L., Andersen, A. S., Gammelgaard, L. K., Sahl, H. G., and Kristensen, H. H. (2010) Plectasin, a fungal defensin, targets the bacterial cell wall precursor Lipid II. *Science* **328,** 1168–1172
37. Sass, V., Schneider, T., Wilmes, M., Körner, C., Tossi, A., Novikova, N., Shamova, O., and Sahl, H. G. (2010) Human β-defensin 3 inhibits cell wall biosynthesis in *Staphylococci*. *Infect. Immun.* **78,** 2793–2800
38. Arnett, E., Lehrer, R. I., Pratikhya, P., Lu, W., and Seveau, S. (2011) Defensins enable macrophages to inhibit the intracellular proliferation of *Listeria monocytogenes*. *Cell Microbiol.* **13,** 635–651
39. Lehrer, R. I., Jung, G., Ruchala, P., Wang, W., Micewicz, E. D., Waring, A. J., Gillespie, E. J., Bradley, K. A., Ratner, A. J., Rest, R. F., and Lu, W.

(2009) Human α-defensins inhibit hemolysis mediated by cholesterol-dependent cytolysins. *Infect. Immun.* **77,** 4028–4040
40. Kim, C., Slavinskaya, Z., Merrill, A. R., and Kaufmann, S. H. (2006) Human α-defensins neutralize toxins of the mono-ADP-ribosyltransferase family. *Biochem. J.* **399,** 225–229
41. Giesemann, T., Guttenberg, G., and Aktories, K. (2008) Human α-defensins inhibit *Clostridium difficile* toxin B. *Gastroenterology* **134,** 2049–2058
42. Jin, T., Bokarewa, M., Foster, T., Mitchell, J., Higgins, J., and Tarkowski, A. (2004) *Staphylococcus aureus* resists human defensins by production of staphylokinase, a novel bacterial evasion mechanism. *J. Immunol.* **172,** 1169–1176
43. Kim, C., Gajendran, N., Mittrücker, H. W., Weiwad, M., Song, Y. H., Hurwitz, R., Wilmanns, M., Fischer, G., and Kaufmann, S. H. (2005) Human α-defensins neutralize anthrax lethal toxin and protect against its fatal consequences. *Proc. Natl. Acad. Sci. U.S.A.* **102,** 4830–4835
44. Mayer-Scholl, A., Hurwitz, R., Brinkmann, V., Schmid, M., Jungblut, P., Weinrauch, Y., and Zychlinsky, A. (2005) Human neutrophils kill *Bacillus anthracis*. *PLoS Pathog.* **1,** e23
45. Wang, W., Mulakala, C., Ward, S. C., Jung, G., Luong, H., Pham, D., Waring, A. J., Kaznessis, Y., Lu, W., Bradley, K. A., and Lehrer, R. I. (2006) Retrocyclins kill bacilli and germinating spores of *Bacillus anthracis* and inactivate anthrax lethal toxin. *J. Biol. Chem.* **281,** 32755–32764
46. Collier, R. J., and Young, J. A. (2003) Anthrax toxin. *Annu. Rev. Cell Dev. Biol.* **19,** 45–70
47. Shoop, W. L., Xiong, Y., Wiltsie, J., Woods, A., Guo, J., Pivnichny, J. V., Felcetto, T., Michael, B. F., Bansal, A., Cummings, R. T., Cunningham, B. R., Friedlander, A. M., Douglas, C. M., Patel, S. B., Wisniewski, D., Scapin, G., Salowe, S. P., Zaller, D. M., Chapman, K. T., Scolnick, E. M., Schmatz, D. M., Bartizal, K., MacCoss, M., and Hermes, J. D. (2005) Anthrax lethal factor inhibition. *Proc. Natl. Acad. Sci. U.S.A.* **102,** 7958–7963
48. Szyk, A., Wu, Z., Tucker, K., Yang, D., Lu, W., and Lubkowski, J. (2006) Crystal structures of human α-defensins HNP4, HD5, and HD6. *Protein Sci.* **15,** 2749–2760
49. Hill, C. P,, Yee, J., Selsted, M. E., and Eisenberg, D. (1991) Crystal structure of defensin HNP-3, an amphiphilic dimer. Mechanisms of membrane permeabilization. *Science* **251,** 1481–1485
50. Ouellette, A. J. (2011) Paneth cell α-defensins in enteric innate immunity. *Cell Mol. Life Sci.* **68,** 2215–2229
51. Maemoto, A., Qu, X., Rosengren, K. J., Tanabe, H., Henschen-Edman, A., Craik, D. J., and Ouellette, A. J. (2004) Functional analysis of the α-defensin disulfide array in mouse cryptdin-4. *J. Biol. Chem.* **279,** 44188–44196
52. Wei, G., de Leeuw, E., Pazgier, M., Yuan, W., Zou, G., Wang, J., Ericksen, B., Lu, W. Y., Lehrer, R. I., and Lu, W. (2009) Through the looking glass, mechanistic insights from enantiomeric human defensins. *J. Biol. Chem.* **284,** 29180–29192
53. Zou, G., de Leeuw, E., Li, C., Pazgier, M., Li, C., Zeng, P., Lu, W. Y., Lubkowski, J., and Lu, W. (2007) Toward understanding the cationicity of defensins. Arg and Lys versus their noncoded analogs. *J. Biol. Chem.* **282,** 19653–19665
54. Tanabe, H., Qu, X., Weeks, C. S., Cummings, J. E., Kolusheva, S., Walsh, K. B., Jelinek, R., Vanderlick, T. K., Selsted, M. E., and Ouellette, A. J. (2004) Structure-activity determinants in paneth cell α-defensins. Loss-of-function in mouse cryptdin-4 by charge-reversal at arginine residue positions. *J. Biol. Chem.* **279,** 11976–11983
55. Wu, Z., Li, X., de Leeuw, E., Ericksen, B., and Lu, W. (2005) Why is the Arg^5–Glu^{13} salt bridge conserved in mammalian α-defensins? *J. Biol. Chem.* **280,** 43039–43047
56. Rajabi, M., de Leeuw, E., Pazgier, M., Li, J., Lubkowski, J., and Lu, W. (2008) The conserved salt bridge in human α-defensin 5 is required for its precursor processing and proteolytic stability. *J. Biol. Chem.* **283,** 21509–21518
57. Rosengren, K. J., Daly, N. L., Fornander, L. M., Jönsson, L. M., Shirafuji, Y., Qu, X., Vogel, H. J., Ouellette, A. J., and Craik, D. J. (2006) Structural and functional characterization of the conserved salt bridge in mammalian paneth cell α-defensins. Solution structures of mouse CRYPTDIN-4 and (E15D)-CRYPTDIN-4. *J. Biol. Chem.* **281,** 28068–28078
58. Andersson, H. S., Figueredo, S. M., Haugaard-Kedström, L. M., Bengtsson, E., Daly, N. L., Qu, X., Craik, D. J., Ouellette, A. J., and Rosengren, K. J. (2012) The α-defensin salt-bridge induces backbone stability to facilitate folding and confer proteolytic resistance. *Amino Acids*, in press
59. Xie, C., Prahl, A., Ericksen, B., Wu, Z., Zeng, P., Li, X., Lu, W. Y., Lubkowski, J., and Lu, W. (2005) Reconstruction of the conserved β-bulge in mammalian defensins using D-amino acids. *J. Biol. Chem.* **280,** 32921–32929
60. Zhao, L., Ericksen, B., Wu, X., Zhan, C., Yuan, W., Li, X., Pazgier, M., and Lu, W. (2012) The invariant Gly residue is important for α-defensin folding, dimerization, and function. A case study of the human neutrophil α-defensin HNP1. *J. Biol. Chem.*, in press
61. Wei, G., Pazgier, M., de Leeuw, E., Rajabi, M., Li, J., Zou, G., Jung, G., Yuan, W., Lu, W. Y., Lehrer, R. I., and Lu, W. (2010) Trp-26 imparts functional versatility to human α-defensin HNP1. *J. Biol. Chem.* **285,** 16275–16285
62. Pazgier, M., Wei, G., Ericksen, B., Jung, G., Wu, Z., de Leeuw, E., Yuan, W., Szmacinski, H., Lu, W. Y., Lubkowski, J., Lehrer, R. I., and Lu, W. (2012) Sometimes it takes two to tango. Contributions of dimerization to functions of human α-defensin HNP1 peptide. *J. Biol. Chem.* **287,** 8944–8953
63. Bevins, C. L., and Salzman, N. H. (2011) Paneth cells, antimicrobial peptides, and maintenance of intestinal homeostasis. *Nat. Rev. Microbiol.* **9,** 356–368
64. de Leeuw, E., Rajabi, M., Zou, G., Pazgier, M., and Lu, W. (2009) Selective arginines are important for the antibacterial activity and host cell interaction of human α-defensin 5. *FEBS Lett.* **583,** 2507–2512
65. de Leeuw, E., Burks, S. R., Li, X., Kao, J. P., and Lu, W. (2007) Structure-dependent functional properties of human defensin 5. *FEBS Lett.* **581,** 515–520
66. Klotman, M. E., Rapista, A., Teleshova, N., Micsenyi, A., Jarvis, G. A., Lu, W., Porter, E., and Chang, T. L. (2008) *Neisseria gonorrhoeae*-induced human defensins 5 and 6 increase HIV infectivity. Role in enhanced transmission. *J. Immunol.* **180,** 6176–6185
67. Wanniarachchi, Y. A., Kaczmarek, P., Wan, A., and Nolan, E. M. (2011) Human defensin 5 disulfide array mutants. Disulfide bond deletion attenuates antibacterial activity against *Staphylococcus aureus*. *Biochemistry* **50,** 8005–8017
68. Rapista, A., Ding, J., Benito, B., Lo, Y. T., Neiditch, M. B., Lu, W., and Chang, T. L. (2011) Human defensins 5 and 6 enhance HIV-1 infectivity through promoting HIV attachment. *Retrovirology* **8,** 45
69. Ding, J., Rapista, A., Teleshova, N., Lu, W., Klotman, M. E., and Chang, T. L. (2011) Mucosal human defensins 5 and 6 antagonize the anti-HIV activity of candidate polyanion microbicides. *J. Innate Immun.* **3,** 208–212
70. Smith, J. G., Silvestry, M., Lindert, S., Lu, W., Nemerow, G. R., and Stewart, P. L. (2010) Insight into the mechanisms of adenovirus capsid disassembly from studies of defensin neutralization. *PLoS Pathog.* **6,** e1000959
71. Chapnik, N., Levit, A., Niv, M. Y., and Froy, O. (2012) Expression and structure/function relationships of human defension 5. *Appl. Biochem. Biotechnol.* **166,** 1703–1710
72. Wu, Z., Ericksen, B., Tucker, K., Lubkowski, J., and Lu, W. (2004) Synthesis and characterization of human α-defensins 4–6. *J. Pept. Res.* **64,** 118–125
73. Pace, C. N., Vajdos, F., Fee, L., Grimsley, G., and Gray, T. (1995) How to measure and predict the molar absorption coefficient of a protein. *Protein Sci.* **4,** 2411–2423
74. Otwinowski, Z., and Minor, W. (1997) Processing of x-ray diffraction data collected in oscillation mode. *Methods Enzymol.* **276,** 307–326
75. Storoni, L. C., McCoy, A. J., and Read, R. J. (2004) Likelihood-enhanced fast rotation functions. *Acta Crystallogr. D Biol. Crystallogr.* **60,** 432–438
76. Murshudov, G. N., Vagin, A. A., and Dodson, E. J. (1997) Refinement of macromolecular structures by the maximum-likelihood method. *Acta Crystallogr. D Biol. Crystallogr.* **53,** 240–255
77. Emsley, P., and Cowtan, K. (2004) Coot. Model-building tools for molecular graphics. *Acta Crystallogr. D Biol. Crystallogr.* **60,** 2126–2132
78. Dawson, P. E., and Kent, S. B. (2000) Synthesis of native proteins by chemical ligation. *Annu. Rev. Biochem.* **69,** 923–960
79. Dawson, P. E., Muir, T. W., Clark-Lewis, I., and Kent, S. B. (1994) Synthesis of proteins by native chemical ligation. *Science* **266,** 776–779
80. Ayabe, T., Satchell, D. P., Pesendorfer, P., Tanabe, H., Wilson, C. L., Hagen, S. J., and Ouellette, A. J. (2002) Activation of Paneth cell α-defensins in mouse small intestine. *J. Biol. Chem.* **277,** 5219–5228

81. Shirafuji, Y., Tanabe, H., Satchell, D. P., Henschen-Edman, A., Wilson, C. L., and Ouellette, A. J. (2003) Structural determinants of procryptdin recognition and cleavage by matrix metalloproteinase-7. *J. Biol. Chem.* **278,** 7910–7919
82. Figueredo, S. M., Weeks, C. S., Young, S. K., and Ouellette, A. J. (2009) Anionic amino acids near the pro-α-defensin N terminus mediate inhibition of bactericidal activity in mouse pro-cryptdin-4. *J. Biol. Chem.* **284,** 6826–6831
83. Wimley, W. C., and White, S. H. (1996) Experimentally determined hydrophobicity scale for proteins at membrane interfaces. *Nat. Struct. Biol.* **3,** 842–848
84. White, S. H., and Wimley, W. C. (1999) Membrane protein folding and stability. Physical principles. *Annu. Rev. Biophys. Biomol. Struct.* **28,** 319–365
85. Bella, J., Hindle, K. L., McEwan, P. A., and Lovell, S. C. (2008) The leucine-rich repeat structure. *Cell Mol. Life Sci.* **65,** 2307–2333
86. Vinson, C., Acharya, A., and Taparowsky, E. J. (2006) Deciphering B-ZIP transcription factor interactions *in vitro* and *in vivo*. *Biochim. Biophys. Acta* **1759,** 4–12
87. Eriksson, A. E., Baase, W. A., Zhang, X. J., Heinz, D. W., Blaber, M., Baldwin, E. P., and Matthews, B. W. (1992) Response of a protein structure to cavity-creating mutations and its relation to the hydrophobic effect. *Science* **255,** 178–183
88. Xu, J., Baase, W. A., Baldwin, E., and Matthews, B. W. (1998) The response of T4 lysozyme to large-to-small substitutions within the core and its relation to the hydrophobic effect. *Protein Sci.* **7,** 158–177
89. Dürr, E., and Jelesarov, I. (2000) Thermodynamic analysis of cavity creating mutations in an engineered leucine zipper and energetics of glycerol-induced coiled coil stabilization. *Biochemistry* **39,** 4472–4482